Int. J. Anal. Appl. (2026), 24:203

International Journal of Analysis and Applications

Unveiling Novel Exact Soliton Structures and Bifurcation Dynamics in the Higher-Order Boussinesq-Burgers Equation via the Modified Extended Mapping Method

Ibrahim Saber[1,2], Hamdy M. Ahmed[3,*], Niveen Badra[1], Islam Samir[1], Mohamed A. Labeeb[2]

[1]*Department of Physics and Mathematics Engineering, Faculty of Engineering, Ain Shams University, Cairo, Egypt*

[2]*Faculty of Artificial Intelligence, Egyptian Russian University, Cairo, Egypt*

[3]*Department of Physics and Engineering Mathematics, Higher Institute of Engineering, El Shorouk Academy, Cairo, Egypt*

[*]*Corresponding author:* hamdy_17eg@yahoo.com

Abstract. This study addresses the challenging problem of deriving exact analytical solutions for the higher-order Boussinesq-Burgers (HOBB) equation, a fundamental nonlinear model that captures complex wave propagation phenomena arising from the intricate interplay between nonlinearity, dispersion, and higher-order effects in various physical contexts, including fluid dynamics and plasma physics. Despite its significance, extracting explicit solutions for such models remains highly nontrivial. To tackle this difficulty, we implement the Modified Extended Mapping Method (MEMM) as a robust and systematic analytical framework. By applying an appropriate traveling wave transformation, the original nonlinear partial differential equation is converted into an ordinary differential equation, which facilitates the derivation of a wide class of exact analytical solutions in explicit form. In parallel, a rigorous bifurcation analysis is conducted to investigate the qualitative behavior of the corresponding dynamical system and to classify the stability properties of its equilibrium states.

1. Introduction

Nonlinear partial differential equations (NLPDEs) represent a central mathematical framework for describing a broad range of complex physical processes where nonlinear effects are predominant. Such interactions arise naturally in many realistic systems where the response is not proportional to the input, leading to rich dynamical behaviors that cannot be captured by linear theories. Although the presence of nonlinearity significantly complicates the derivation of exact solutions, it

Received: May 1, 2026.

2020 *Mathematics Subject Classification.* 35C08, 35Q51, 37G10.

Key words and phrases. higher-order nonlinear effects; nonlinear wave dynamics; bifurcation analysis; wave propagation in fluids and plasmas; solitons.

https://doi.org/10.28924/2291-8639-24-2026-203
ISSN: 2291-8639

simultaneously enables the emergence of remarkable physical structures such as solitons, wave localization, and pattern formation. Such characteristics render NLPDEs essential for modeling nonlinear phenomena across various disciplines, including fluid dynamics, plasma physics, nonlinear optics, and condensed matter physics [1].

From a physical perspective, Solitons are stable, localized wave structures that maintain their form and propagation speed as a result of a precise balance between nonlinear effects and dispersion. This balance is a central concept in nonlinear science and has been reported in numerous experimental settings, for instance, waves propagating in shallow water regions, optical fibers and plasma environments. Consequently, the construction of exact analytical solutions is not only of mathematical interest and simultaneously provides important insights into the fundamental physical mechanisms governing these systems.

To address the inherent complexity of NLPDEs, a wide range of analytical techniques has been developed. Among the most effective methods are the Kudryashov method [2,3], the Exp-function method [4], the $(G'/G, 1/G)$-expansion method [5–7], and the extended tanh-function method [8–10]. These approaches have proven successful in generating diverse classes of exact solutions, including solitary waves, periodic structures, and singular solutions, thereby contributing significantly to the qualitative and quantitative understanding of nonlinear wave propagation.

The Higher-Order Boussinesq–Burgers equation (HOBB) represents an important physical model that describes the propagation of nonlinear dispersive waves in media where higher-order nonlinear and dissipative effects cannot be neglected. This equation extends the classical Boussinesq–Burgers model originally proposed by Zhang [11], incorporating additional terms that account for complex interactions such as wave steepening, higher-order dispersion, and nonlinear coupling between wave components. These effects are particularly relevant in fluid flow, plasma dynamics, and nonlinear optical media, where wave evolution is governed by competing physical mechanisms.

The governing system is

$$\begin{cases} u_t - 3gu^2u_x + \frac{3}{2}g(uv)_x - \frac{1}{4}gu_{xxx} = 0, \\ v_t + \frac{3}{2}gvv_x - 3g(u^2v)_x + 3gu_xu_{xx} + \frac{3}{2}guu_{xxx} - \frac{1}{4}gv_{xxx} = 0, \end{cases} \tag{1.1}$$

for which $u = u(x,t)$ and $v = v(x,t)$ represent the wave amplitudes, and $g \in \mathbb{R} \setminus \{0\}$ is a constant parameter controlling the strength of nonlinearity and dispersion. Physically, the interaction between the two fields u and v reflects coupled wave dynamics, which may correspond to multi-component wave propagation in complex media.

In recent years, the HOBB model has attracted considerable attention due to its ability to capture a wide range of nonlinear wave phenomena. Zhang [11] derived quasi-periodic solutions using the nonlinearization method, while Zuo and Zhang [12] applied the Hirota bilinear technique to construct soliton solutions. Wazwaz [13] further extended this framework to obtain both periodic and solitary wave structures. Additional contributions include the work of Guo [14], who employed the extended homogeneous balance method to generate multi-soliton solutions, and Zafar [15], who

introduced fractional-order effects to model shallow water dynamics more accurately. Furthermore, Jaradat [16] revisited the model using a simplified bilinear approach, whereas Gao [17] utilized symbolic computation to derive Bäcklund transformations. The symmetry properties of the system were investigated by Liu [18], leading to invariant solutions of various functional forms, while Mubaraki [19] combined analytical and computational techniques to obtain exact solutions along with their graphical representations.

Motivated by the above developments, the present study introduces, for the first time, the application of the Modified Extended Mapping Method (MEMM) and its generalized forms to the HOBB equation. This approach enables the systematic construction of a rich spectrum of new exact solutions, including physically relevant wave structures that have not been reported previously.

To further deepen the physical interpretation of the obtained solutions, bifurcation theory is employed as a powerful analytical tool. This framework allows for a detailed investigation of equilibrium states and their stability, providing insight into transitions between different dynamical regimes as system parameters vary. Such analysis is crucial for gaining insight into the qualitative dynamics of nonlinear waves and their stability under realistic physical conditions.

The rest of this paper is structured as follows. Section 2 introduces the theoretical framework of the Modified Extended Mapping Method along with its extensions. Section 3 focuses on constructing exact solutions. In Section 4, the physical properties of the obtained solutions are demonstrated using three-dimensional graphical representations. Section 5 presents a detailed bifurcation analysis, while Section 6 concludes the study by summarizing the main findings and outlining potential directions for future work.

2. Exploration of Exact Solutions using MEMM

This segment outlines the fundamental principles of the augmented Modified Extended Mapping technique, as documented in [20–22]. To illustrate the procedure, consider the following representation of a nonlinear differential equation of partial type (NLPDE):

$$F\left(f, f_x, f_t, f_{xt}, f_{xx}, f_{xxx} \ldots\right) = 0. \tag{2.1}$$

To construct the analytical solutions of Eq. (2.1) through the modified extended mapping framework, the following systematic procedure is implemented:

Step(1): At the outset, the governing NLPDE presented in Eq. (2.1) is reduced into a nonlinear ordinary differential equation (ODE). This reduction is achieved by introducing a suitable wave transformation of the form:

$$f(x,t) = f(\xi),\ \xi = x - c\,t,\ c \neq 0, \tag{2.2}$$

in this context, c denotes a real constant signifying the velocity of the wave. Consequently, the application of this transformation reduces Eq. (2.1) to the following form:

$$H\left(f, f', f'', f''', \ldots\right) = 0 \tag{2.3}$$

Step(2): We assume an ansatz for the solution of Eq. (2.3) as follows:

$$f(\xi) = \sum_{j=0}^{N} a_j z^j(\xi) + \sum_{j=-1}^{-N} b_{-j} z^j(\xi) + \sum_{j=2}^{N} c_j z^{j-2}(\xi) z'(\xi) + \sum_{j=-1}^{-N} d_{-j} z^j(\xi) z'(\xi). \tag{2.4}$$

where a_j, b_{-j}, c_j, d_{-j} denote real-valued coefficients to be determined, while $z(\xi)$ is governed by the following auxiliary equation:

$$z'(\xi) = \sqrt{\sigma_0 + \sigma_1 z(\xi) + \sigma_2 z^2(\xi) + \sigma_3 z^3(\xi) + \sigma_4 z^4(\xi) + \sigma_6 z^6(\xi)}. \tag{2.5}$$

Step (3): The value of the positive integer N is evaluated by applying the principle of homogeneous balance. This involves equilibrating the highest-order linear differential term with the highest-order nonlinear component present in Eq. (2.3).

Step(4): By substituting the proposed ansatz from Eq. (2.4) and its derivatives—incorporating the auxiliary condition in Eq. (2.5)—into the reduced ODE, we obtain a complex expression in terms of $z(\xi)$. By systematically collecting and setting the coefficients of $z'^j(\xi) z^i(\xi)$ (for $j = 0, 1$ and $i = 0, \pm 1, \pm 2, \ldots$) to zero, a comprehensive system of algebraic equations is constructed for the unknown parameters a_j, b_{-j}, c_j, d_{-j}, and c.

Step (5): To manage the complexity of the resulting algebraic system, the Mathematica software package is employed. Solving this system allows for the precise determination of the constants a_j, b_{-j}, c_j, and d_{-j}.

Step(6): A diverse array of exact solution types can be retrieved by substituting various combinations of the structural parameters $\sigma_0, \sigma_1, \sigma_2, \sigma_3, \sigma_4$, and σ_6 into the general form. The specific cases are categorized as follows:

Case 1: $\sigma_0 = \sigma_1 = \sigma_3 = \sigma_6 = 0$

$$z(\xi) = \sqrt{-\frac{\sigma_2}{\sigma_4}} \operatorname{sech}\left(\sqrt{\sigma_2}\xi\right), \quad \sigma_2 > 0, \sigma_4 < 0.$$

$$z(\xi) = \sqrt{-\frac{\sigma_2}{\sigma_4}} \sec\left(\sqrt{-\sigma_2}\xi\right), \quad \sigma_2 < 0, \sigma_4 > 0.$$

$$z(\xi) = \sqrt{-\frac{\sigma_2}{\sigma_4}} \operatorname{csc}\left(\sqrt{-\sigma_2}\xi\right), \quad \sigma_2 < 0, \sigma_4 > 0.$$

Case 2: $\sigma_0 = \sigma_1 = \sigma_2 = \sigma_6 = 0$

$$z(\xi) = \frac{4\sigma_3}{\sigma_3^2(\xi)^2 - 4\sigma_4}.$$

Case 3: $\sigma_0 = \sigma_1 = \sigma_6 = 0$

$$z(\xi) = -\frac{\sigma_2\left(\tanh\left(\frac{1}{2}\sqrt{\sigma_2}\xi\right) + 1\right)}{\sigma_3}, \quad \sigma_3^2 = 4\sigma_2\sigma_4, \sigma_2 > 0.$$

$$z(\xi) = -\frac{\sigma_2\left(\coth\left(\frac{1}{2}\sqrt{\sigma_2}(x - vt)\right) + 1\right)}{\sigma_3}, \quad \sigma_3^2 = 4\sigma_2\sigma_4, \sigma_2 > 0.$$

Case 4: $\sigma_1 = \sigma_3 = \sigma_6 = 0$

No.	σ_0	σ_2	σ_4	$z(\xi)$
1	m^2-1	$-m^2+2$	-1	$dn(\xi,m)$
2	$m^2-2m^3+m^4$	$-\frac{4}{m}$	$-1+6m-m^2$	$\frac{m\,\mathrm{dn}(\xi\|m)\,\mathrm{cn}(\xi\|m)}{1+m\,\mathrm{sn}(\xi\|m)^2}$

Upon substituting the evaluated parameters and the specific forms of $z(\xi)$ back into the hypothesized solution, we can retrieve an extensive variety of solitary wave solutions and other exact analytical expressions for the governing NLPDE.

3. The Exact Wave Solutions

In this part of the study, an array of Exact analytical solutions of Eq. (1.1) are developed using an augmented mapping approach. By utilizing a traveling wave transformation $u(x,t) = f(\xi)$, $v(x,t) = h(\xi)$ with $\xi = x - ct$, we first establish the balancing numbers for the system. The substitution of this transformation into Eq. (1.1) results in the subsequent ordinary differential equations:

$$\begin{cases} -cf' - \frac{1}{4}f^{(3)}g + \frac{3}{2}g\,(hf' + fh') - 3f^2gf' = 0, \\ -ch' + \frac{3}{2}ff^{(3)}g - 3g\left(f^2h' + 2fhf'\right) + 3gf'f'' - \frac{1}{4}gh^{(3)} + \frac{3}{2}ghh' = 0. \end{cases} \tag{3.1}$$

by getting relation between h,f by putting $h(\xi) = \rho f(\xi)$we can obtain:

$$\begin{cases} -cf' + 3g\rho ff' - 3gf^2f' - \frac{1}{4}gf''' = 0, \\ -cf' + \frac{3}{2}g\rho^2ff' - 9g\rho f^2f' + 3gf'f'' - \frac{1}{4}g\rho f''' + \frac{3}{2}gff''' = 0. \end{cases} \tag{3.2}$$

We can write both equations in a single equation as if we multiply first equation in system (3.2) by $(\rho - 3f)$ and solving the system, it gives the following ODE:

$$-c\,f - \frac{1}{4}g\,f'' + \frac{3}{2}g\rho f^2 - g\,f^3 = 0. \tag{3.3}$$

Equilibrating the highest-order derivative f'' with the cubic nonlinear term f^3 in Eq. (3.3) leads to a balancing index of $N = 1$. Accordingly, the solution for Eq. (3.2) can be formulated in the manner described below:

$$f(\xi) = a_0 + a_1 z + \frac{b_1}{z} + d_1\frac{z'}{z}. \tag{3.4}$$

By substituting the proposed ansatz in Eq. (3.2) and the auxiliary condition in Eq. (2.5) into Eq. (3.2), we extract a series of terms in ${z'}^j z^i$.Imposing zero conditions on the respective coefficients results in an algebraic system that is subsequently solved using the Mathematica symbolic computation package, leading to the following sets of parameters:

Case 1:. When $\sigma_0 = \sigma_1 = \sigma_3 = \sigma_6 = 0$, The subsequent results are established:

Set I:

$$a_0 = 0; \sigma_4 = -2a_1^2; b_1 = 0; d_1 = 0; \sigma_2 = -\frac{4c}{g}; \rho = 0.$$

Set II

$$a_0 = -\frac{\sqrt{\sigma_2}}{2}; \sigma_4 = -2a_1; b_1 = 0; d_1 = 0; \sigma_2 = \frac{2c}{g}; \rho = -\sqrt{\sigma_2}.$$

Set III

$$a_0 = \frac{\sqrt{\sigma_2}}{2}; \sigma_4 = -2a_1^2; b_1 = 0; d_1 = 0; \sigma_2 = \frac{2c}{g}; \rho = \sqrt{\sigma_2}.$$

According to Set I, leading to the bright soliton solutions:

$$u(x,t) = \sqrt{2}\sqrt{-\frac{c}{g}}\operatorname{sech}\left(2\sqrt{-\frac{c}{g}}(x-ct)\right), \frac{c}{g} < 0, \tag{3.5}$$

$$v(x,t) = \sqrt{2}\rho\sqrt{-\frac{c}{g}}\operatorname{sech}\left(2\sqrt{-\frac{c}{g}}(x-ct)\right), \frac{c}{g} < 0. \tag{3.6}$$

According to Set II, leading to the bright soliton solutions:

$$u(x,t) = \sqrt{\frac{c}{g}}\operatorname{sech}\left(\sqrt{2}\sqrt{\frac{c}{g}}(x-ct)\right) - \frac{1}{\sqrt{2}}\sqrt{\frac{c}{g}}, \frac{c}{g} > 0, \tag{3.7}$$

$$v(x,t) = \rho\sqrt{\frac{c}{g}}\operatorname{sech}\left(\sqrt{2}\sqrt{\frac{c}{g}}(x-ct)\right) - \frac{\rho}{\sqrt{2}}\sqrt{\frac{c}{g}}, \frac{c}{g} > 0. \tag{3.8}$$

According to Set III, leading to the bright soliton solutions:

$$u(x,t) = \sqrt{\frac{c}{g}}\operatorname{sech}\left(\sqrt{2}\sqrt{\frac{c}{g}}(x-ct)\right) + \frac{1}{\sqrt{2}}\sqrt{\frac{c}{g}}, \frac{c}{g} > 0, \tag{3.9}$$

$$u(x,t) = \rho\sqrt{\frac{c}{g}}\operatorname{sech}\left(\sqrt{2}\sqrt{\frac{c}{g}}(x-ct)\right) + \frac{\rho}{\sqrt{2}}\sqrt{\frac{c}{g}}, \frac{c}{g} > 0. \tag{3.10}$$

Case 2:. When $\sigma_0 = \sigma_1 = \sigma_2 = \sigma_6 = 0$, The resulting outcomes are:

Set I

$$a_0 = -\frac{3\sigma_3}{4\sqrt{-2\sigma_4}}; \sigma_4 = -2a_1^2; b_1 = 0; d_1 = 0; g = -\frac{32c\sigma_4}{9\sigma_3^2}; \sigma_3 = -\rho\sqrt{-2\sigma_4}.$$

Set II

$$a_0 = \frac{3\sigma_3}{4\sqrt{-2\sigma_4}}; \sigma_4 = -2a_1^2; b_1 = 0; d_1 = 0; g = -\frac{32c\sigma_4}{9\sigma_3^2}; \sigma_3 = \rho\sqrt{-2\sigma_4}.$$

According to Set I, the following rational solution are raised:

$$u(x,t) = \frac{3\rho}{4} - \frac{8\rho}{4\rho^2(x-ct)^2+8}, \tag{3.11}$$

$$v(x,t) = \frac{3\rho^2}{4} - \frac{8\rho^2}{4\rho^2(x-ct)^2+8}. \tag{3.12}$$

According to Set II, the following rational solution is raised:

$$u(x,t) = \frac{8\rho}{4\rho^2(x-ct)^2+8} + \frac{3\rho}{4}, \tag{3.13}$$

$$v(x,t) = \frac{8\rho^2}{4\rho^2(x-ct)^2+8} + \frac{3\rho^2}{4}. \tag{3.14}$$

Case 3 When $\sigma_0 = \sigma_1 = \sigma_6 = 0$, The resulting outcomes are:

Set I

$$a_0 = 0; \sigma_4 = -2a_1^2; b_1 = 0; d_1 = 0; \sigma_2 = -\frac{4c}{g}; \rho = \frac{\sqrt{-4\sigma_2\sigma_4}}{2\sqrt{2}\sqrt{\sigma_4}}.$$

According to Set I, the following (dark, singular) soliton solutions are raised:

$$u(x,t) = \frac{c\left(\tanh\left(\sqrt{-\frac{c}{g}}(x-ct)\right)+1\right)}{\sqrt{2}g\sqrt{-\frac{c}{g}}}, \frac{c}{g} < 0, \tag{3.15}$$

$$v(x,t) = \frac{\rho\, c\left(\tanh\left(\sqrt{-\frac{c}{g}}(x-ct)\right)+1\right)}{\sqrt{2}\, g\sqrt{-\frac{c}{g}}}, \frac{c}{g} < 0. \tag{3.16}$$

$$u(x,t) = \frac{c\left(\coth\left(\sqrt{-\frac{c}{g}}(x-ct)\right)+1\right)}{\sqrt{2}g\sqrt{-\frac{c}{g}}}, \frac{c}{g} < 0, \tag{3.17}$$

$$v(x,t) = \frac{\rho\, c\left(\coth\left(\sqrt{-\frac{c}{g}}(x-ct)\right)+1\right)}{\sqrt{2}\, g\sqrt{-\frac{c}{g}}}, \frac{c}{g} < 0. \tag{3.18}$$

Case 4.1

Set I

$$a_0 = 0; a_1 = -\frac{1}{\sqrt{2}}; b_1 = 0; d_1 = 0; c = \frac{4g}{m^2-2}; \rho = 0.$$

Set II

$$a_0 = 0; a_1 = \frac{1}{\sqrt{2}}; b_1 = 0; d_1 = 0; c = \frac{4g}{m^2-2}; \rho = 0.$$

Set III

$$a_0 = -\frac{1}{2}\sqrt{2-m^2}; a_1 = -\frac{1}{\sqrt{2}}; b_1 = 0; d_1 = 0; c = -\frac{2g}{m^2-2}; \rho = -\sqrt{2-m^2}.$$

Set IV

$$a_0 = \frac{\sqrt{2-m^2}}{2}; a_1 = -\frac{1}{\sqrt{2}}; b_1 = 0; d_1 = 0; c = -\frac{2g}{m^2-2}; \rho = \sqrt{2-m^2}.$$

According to Set I, leading to the bright soliton solutions:

$$u(x,t) = -\frac{\mathrm{dn}\left(\frac{4gt}{m^2-2} - x\middle| m\right)}{\sqrt{2}}. \tag{3.19}$$

at m=1

$$u(x,t) = -\frac{\mathrm{sech}(4gt+x)}{\sqrt{2}}. \tag{3.20}$$

$$v(x,t) = -\frac{\rho \, \mathrm{dn}\left(\frac{4gt}{m^2-2} - x \middle| m\right)}{\sqrt{2}}. \tag{3.21}$$

at m=1

$$v(x,t) = -\frac{\rho \, \mathrm{sech}(4gt + x)}{\sqrt{2}}. \tag{3.22}$$

According to Set II, leading to the bright soliton solutions:

$$u(x,t) = \frac{\mathrm{dn}\left(\frac{4gt}{m^2-2} - x \middle| m\right)}{\sqrt{2}}. \tag{3.23}$$

at m=1

$$u(x,t) = \frac{\mathrm{sech}(4gt + x)}{\sqrt{2}}. \tag{3.24}$$

$$v(x,t) = \frac{\rho \, \mathrm{dn}\left(\frac{4gt}{m^2-2} - x \middle| m\right)}{\sqrt{2}}. \tag{3.25}$$

at m=1

$$v(x,t) = \frac{\rho \, \mathrm{sech}(4gt + x)}{\sqrt{2}}. \tag{3.26}$$

According to Set III, leading to the bright soliton solutions:

$$u(x,t) = -\frac{\mathrm{dn}\left(\frac{4gt}{m^2-2} + x \middle| m\right)}{\sqrt{2}} - \frac{\sqrt{2-m^2}}{2}, \; 2 - m^2 > 0. \tag{3.27}$$

at m=1

$$u(x,t) = -\frac{\mathrm{sech}(4gt - x)}{\sqrt{2}} - \frac{1}{2}, \tag{3.28}$$

$$v(x,t) = -\frac{\rho \, \mathrm{dn}\left(\frac{4gt}{m^2-2} + x \middle| m\right)}{\sqrt{2}} - \frac{\rho \, \sqrt{2-m^2}}{2}, \; 2 - m^2 > 0, \tag{3.29}$$

at m=1

$$v(x,t) = -\frac{\rho \, \mathrm{sech}(4gt - x)}{\sqrt{2}} - \frac{\rho}{2}. \tag{3.30}$$

According to Set IV, leading to the bright soliton solutions:

$$u(x,t) = \frac{\sqrt{2-m^2}}{2} - \frac{\mathrm{dn}\left(\frac{4gt}{m^2-2} + x \middle| m\right)}{\sqrt{2}}, \; 2 - m^2 > 0. \tag{3.31}$$

at m=1

$$u(x,t) = \frac{1}{2} - \frac{\mathrm{sech}(4gt - x)}{\sqrt{2}}, \tag{3.32}$$

$$v(x,t) = \frac{\rho\ \sqrt{2-m^2}}{2} - \frac{\rho\ \mathrm{dn}\left(\frac{4gt}{m^2-2} + x\middle| m\right)}{\sqrt{2}},\ 2-m^2 > 0. \tag{3.33}$$

at m=1

$$v(x,t) = \frac{\rho}{2} - \frac{\rho\ \mathrm{sech}(4gt-x)}{\sqrt{2}}. \tag{3.34}$$

Case 4.2

Set I

$$a_0 = -\sqrt{-\frac{1}{m}}; a_1 = -\frac{\sqrt{m^2-6m+1}}{\sqrt{2}}; b_1 = 0; d_1 = 0; c = -\frac{1}{2}(gm); \rho = -2\sqrt{-\frac{1}{m}}.$$

Set II

$$a_0 = -\sqrt{-\frac{1}{m}}; a_1 = \frac{\sqrt{m^2-6m+1}}{\sqrt{2}}; b_1 = 0; d_1 = 0; c = -\frac{1}{2}(gm); \rho = -2\sqrt{-\frac{1}{m}}.$$

Set III

$$a_0 = \sqrt{-\frac{1}{m}}; a_1 = -\frac{\sqrt{m^2-6m+1}}{\sqrt{2}}; b_1 = 0; d_1 = 0; c = -\frac{1}{2}(gm); \rho = 2\sqrt{-\frac{1}{m}}.$$

Set IV

$$a_0 = 0; a_1 = -\frac{\sqrt{m^2-6m+1}}{\sqrt{2}}; b_1 = 0; d_1 = 0; c = \mathrm{gm}; \rho = 0.$$

Set V

$$a_0 = 0; a_1 = \frac{\sqrt{m^2-6m+1}}{\sqrt{2}}; b_1 = 0; d_1 = 0; c = \mathrm{gm}; \rho = 0.$$

According to Set I, leading to the bright soliton solutions:

$$u(x,t) = -\frac{m\sqrt{m^2-6m+1}\mathrm{cn}\left(\frac{gmt}{2} + x\middle| m\right)\mathrm{dn}\left(\frac{gmt}{2} + x\middle| m\right)}{\sqrt{2}\left(m\mathrm{sn}\left(\frac{gmt}{2} + x\middle| m\right)^2 + 1\right)} - \sqrt{-\frac{1}{m}},\ \frac{1}{m} < 0. \tag{3.35}$$

at m=1

$$u(x,t) = -\sqrt{-\left(\sqrt{2}\mathrm{sech}(gt+2x)+1\right)}, \left(\sqrt{2}\mathrm{sech}(gt+2x)+1\right) < 0. \tag{3.36}$$

$$v(x,t) = -\frac{\rho\ m\sqrt{m^2-6m+1}\mathrm{cn}\left(\frac{gmt}{2} + x\middle| m\right)\mathrm{dn}\left(\frac{gmt}{2} + x\middle| m\right)}{\sqrt{2}\left(m\mathrm{sn}\left(\frac{gmt}{2} + x\middle| m\right)^2 + 1\right)} - \rho\ \sqrt{-\frac{1}{m}},\ \frac{1}{m} < 0. \tag{3.37}$$

at m=1

$$v(x,t) = -\rho\ \sqrt{-\left(\sqrt{2}\mathrm{sech}(gt+2x)+1\right)}, \left(\sqrt{2}\mathrm{sech}(gt+2x)+1\right) < 0. \tag{3.38}$$

According to Set II, leading to the bright soliton solutions:

$$u(x,t)=\frac{m\sqrt{m^2-6m+1}\mathrm{cn}\left(\frac{gmt}{2}+x\middle|m\right)\mathrm{dn}\left(\frac{gmt}{2}+x\middle|m\right)}{\sqrt{2}\left(m\mathrm{sn}\left(\frac{gmt}{2}+x\middle|m\right)^2+1\right)}-\sqrt{-\frac{1}{m}},\ \frac{1}{m}<0. \tag{3.39}$$

at m=1

$$u(x,t)=-\sqrt{-\left(\sqrt{2}\mathrm{sech}(gt+2x)-1\right)},\left(\sqrt{2}\mathrm{sech}(gt+2x)-1\right)<0. \tag{3.40}$$

$$v(x,t)=\frac{\rho\, m\sqrt{m^2-6m+1}\mathrm{cn}\left(\frac{gmt}{2}+x\middle|m\right)\mathrm{dn}\left(\frac{gmt}{2}+x\middle|m\right)}{\sqrt{2}\left(m\mathrm{sn}\left(\frac{gmt}{2}+x\middle|m\right)^2+1\right)}-\rho\sqrt{-\frac{1}{m}},\ \frac{1}{m}<0. \tag{3.41}$$

at m=1

$$v(x,t)=-\rho\sqrt{-\left(\sqrt{2}\mathrm{sech}(gt+2x)-1\right)},\left(\sqrt{2}\mathrm{sech}(gt+2x)-1\right)<0. \tag{3.42}$$

According to Set III, leading to the bright soliton solutions:

$$u(x,t)=-\frac{m\sqrt{m^2-6m+1}\mathrm{cn}\left(\frac{gmt}{2}+x\middle|m\right)\mathrm{dn}\left(\frac{gmt}{2}+x\middle|m\right)}{\sqrt{2}\left(m\mathrm{sn}\left(\frac{gmt}{2}+x\middle|m\right)^2+1\right)}+\sqrt{-\frac{1}{m}},\ \frac{1}{m}<0. \tag{3.43}$$

at m=1

$$u(x,t)=\sqrt{-\left(\sqrt{2}\mathrm{sech}(gt+2x)+1\right)},\left(\sqrt{2}\mathrm{sech}(gt+2x)-1\right)<0. \tag{3.44}$$

$$v(x,t)=-\frac{\rho\, m\sqrt{m^2-6m+1}\mathrm{cn}\left(\frac{gmt}{2}+x\middle|m\right)\mathrm{dn}\left(\frac{gmt}{2}+x\middle|m\right)}{\sqrt{2}\left(m\mathrm{sn}\left(\frac{gmt}{2}+x\middle|m\right)^2+1\right)}+\rho\sqrt{-\frac{1}{m}},\ \frac{1}{m}<0. \tag{3.45}$$

at m=1

$$v(x,t)=\rho\ \sqrt{-\left(\sqrt{2}\mathrm{sech}(gt+2x)+1\right)},\left(\sqrt{2}\mathrm{sech}(gt+2x)-1\right)<0. \tag{3.46}$$

According to Set IV, leading to the bright soliton solutions:

$$u(x,t)=-\frac{m\sqrt{m^2-6m+1}\mathrm{cn}(\mathrm{gm}t-x|m)\mathrm{dn}(\mathrm{gm}t-x|m)}{\sqrt{2}\,(m\mathrm{sn}(\mathrm{gm}t-x|m)^2+1)}. \tag{3.47}$$

at m=1

$$u(x,t)=-\sqrt{-2\mathrm{sech}^2(2\mathrm{gm}t-2x)},\ 2\mathrm{sech}(2gmt+2x)<0. \tag{3.48}$$

$$v(x,t)=-\frac{\rho\, m\sqrt{m^2-6m+1}\mathrm{cn}(\mathrm{gm}t-x|m)\mathrm{dn}(\mathrm{gm}t-x|m)}{\sqrt{2}\,(m\mathrm{sn}(\mathrm{gm}t-x|m)^2+1)}. \tag{3.49}$$

at m=1

$$v(x,t)=-\rho\sqrt{-2\mathrm{sech}^2(2\mathrm{gm}t-2x)},\ 2\mathrm{sech}(2gmt+2x)<0. \tag{3.50}$$

According to Set V, leading to the bright soliton solutions:

$$u(x,t) = \frac{m\sqrt{m^2-6m+1}\text{cn}(\text{gm}t-x|m)\text{dn}(\text{gm}t-x|m)}{\sqrt{2}\,(m\text{sn}(\text{gm}t-x|m)^2+1)}. \tag{3.51}$$

at m=1

$$u(x,t) = \sqrt{-2\text{sech}^2(2\text{gm}t-2x)},\ 2\text{sech}(2gmt+2x) < 0. \tag{3.52}$$

$$v(x,t) = \frac{\rho\, m\sqrt{m^2-6m+1}\text{cn}(\text{gm}t-x|m)\text{dn}(\text{gm}t-x|m)}{\sqrt{2}\,(m\text{sn}(\text{gm}t-x|m)^2+1)}. \tag{3.53}$$

at m=1

$$v(x,t) = \rho\ \sqrt{-2\text{sech}^2(2\text{gm}t-2x)},\ 2\text{sech}^2(2gmt+2x) < 0. \tag{3.54}$$

4. Evaluation of Bifurcation Analysis

Bifurcation analysis investigates qualitative shifts in dynamical system behavior triggered by parameter variations. In nonlinear frameworks, minor perturbations can induce fundamental changes in stability or equilibrium states. These critical thresholds, or bifurcations, often mark the onset of oscillatory patterns, chaotic dynamics, or multistability [23,24].

In the context of Eq. (3.3), the problem may be equivalently expressed in the following form:

$$f'' = \frac{4c}{g}f - 6\rho f^2 + 4f^3. \tag{4.1}$$

To reformulate the second-order model as a planar system, we employ the transformation $f' = y$, yielding the subsequent first-order differential equations:

$$\begin{cases} f' = y, \\ y' = \frac{4c}{g}f - 6\rho f^2 + 4f^3. \end{cases} \tag{4.2}$$

Stationary points $E(f,y) \in \{(0,0),(f_1,0),(f_2,0)\}$ are obtained by vanishing the derivatives in Eq. (4.2). The stability of these points is governed by the Jacobian matrix:

$$J = \begin{pmatrix} \frac{\partial f}{\partial H} & \frac{\partial f}{\partial q} \\ \frac{\partial g}{\partial H} & \frac{\partial g}{\partial q} \end{pmatrix} = \begin{pmatrix} 0 & 1 \\ \frac{4c}{g}f - 6\rho f^2 + 4f^3 & 0 \end{pmatrix}$$

where $l_1(f,y) = y$ while $l_2(f,y) = 4f^2 - 6\rho f + \frac{4c}{g}$ The eigenvalues associated with the linear transformation J are:

$$\lambda = \pm\sqrt{4f^2 - 6\rho f + \frac{4c}{g}},\ f_{1,2} = \frac{6\rho \pm \sqrt{36\rho^2 - 64\frac{c}{g}}}{8}. \tag{4.3}$$

Stability at (0,0)

The classification of equilibrium states depends fundamentally on the sign of the parameter $\frac{4c}{g}$

- When $\frac{4c}{g} > 0$, the point is an unstable saddle due to the presence of real eigenvalues with opposing signs.

- When $\frac{4c}{g} < 0$, the system exhibits purely imaginary eigenvalues, identifying the equilibrium as a neutrally stable center.

Therefore, a qualitative change in the phase portrait occurs when $\frac{4c}{g} = 0$, which indicates the presence of a bifurcation in the dynamical system.

Stability at ($f_{1,2}$,0) The equilibrium points of the system are given $(f_1, 0)$ and $(f_2, 0)$

- If $36\rho^2 - 64\frac{c}{g} < 0$, the point is a center surrounded by closed orbits.
- If $36\rho^2 - 64\frac{c}{g} > 0$, the point is a saddle with separatrix structure.

5. Graphical Analysis and Discussion

This section provides a visual interpretation of the physical properties of the obtained solutions and explores the global dynamics of the system.

- **Figures (1)–(4):** Illustrate the spatial-temporal evolution of several wave structures:
  - **Fig. 1:** Represents a **bright soliton** profile for Eq. (3.5) with parameters $c = 0.155$, $g = -0.5$.
  - **Fig. 2:** Displays a **singular soliton** configuration from Eq. (3.17) taking $c = 0.08$, $g = -4$.
  - **Fig. 3:** Shows a **dark soliton** solution based on Eq. (3.15) for $c = 0.3$, $g = -0.3$.
  - **Fig. 4:** Depicts a **Rational solution** pattern arising from Eq. (3.11) at $c = 0$, $g = 1.16$.
- **Figures (5)–(6):** Exhibit the **phase portraits** which characterize the qualitative dynamics of the planar system:
  - **Fig. 5:** Phase trajectories at $\rho = 1$: (a) Stable **center** behavior ($c = 0.155, g = -0.5$), and (b) Unstable **saddle** point ($c = 0.155, g = 0.5$).
  - **Fig. 6:** Phase trajectories at $\rho = 1$: (a) Stable **center** behavior ($c = 0.1, g = -0.4$), and (b) Unstable **saddle** point ($c = 0.1, g = 0.4$).

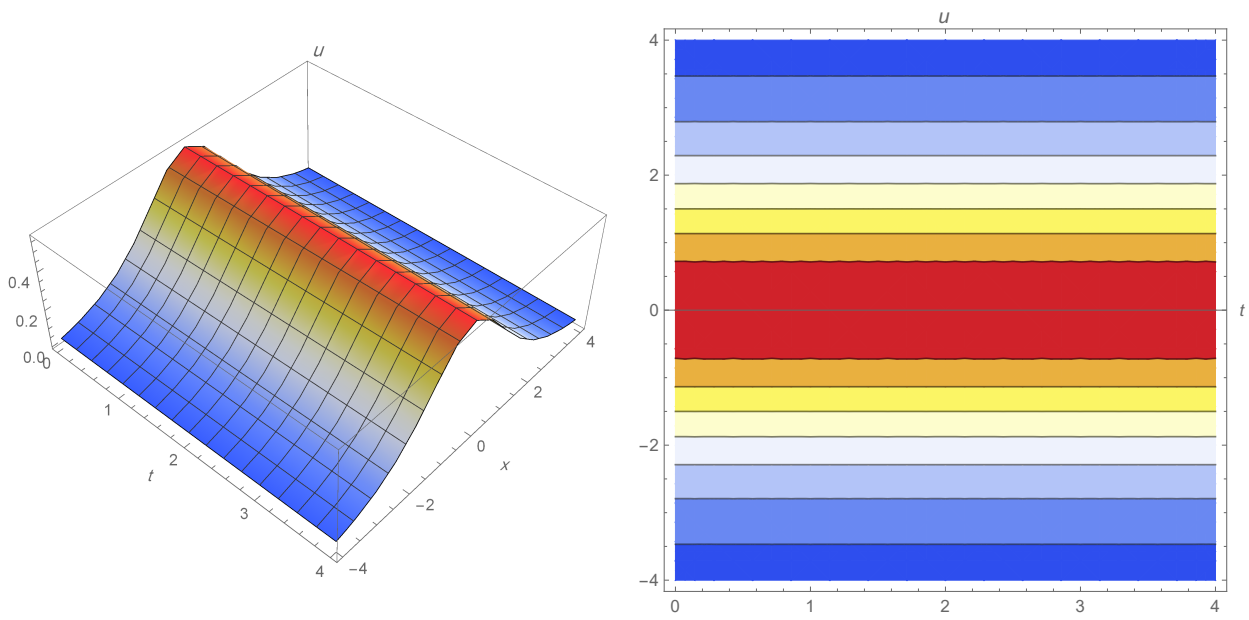

Figure (1): Bright soliton of Eq.(3.5).

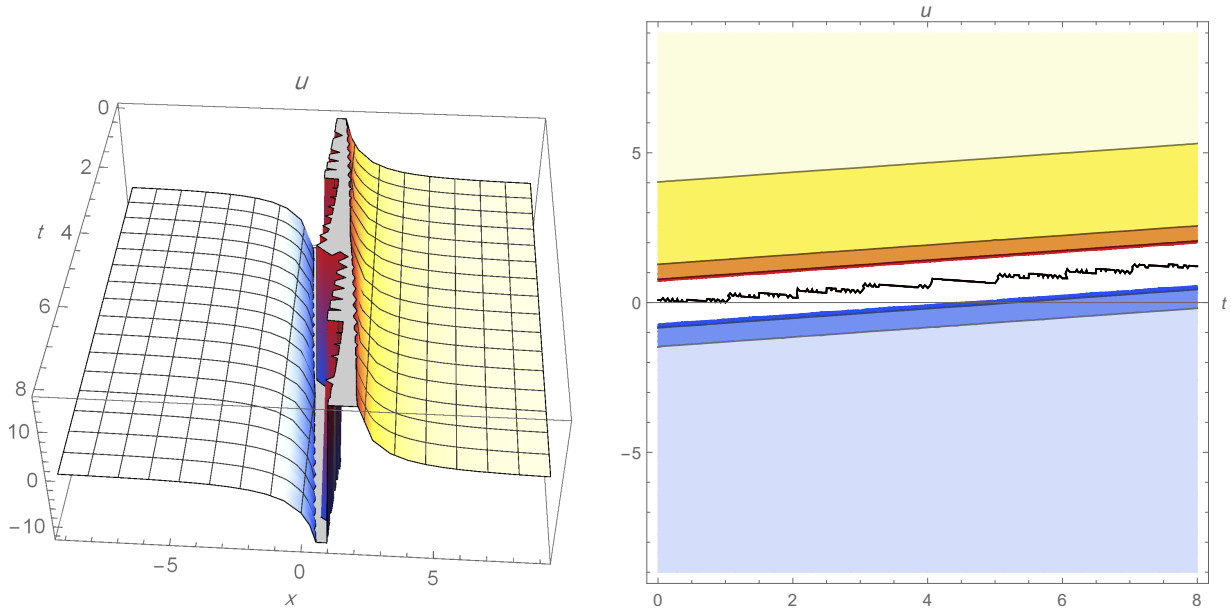

Figure (2): Singular soliton of Eq.(3.17).

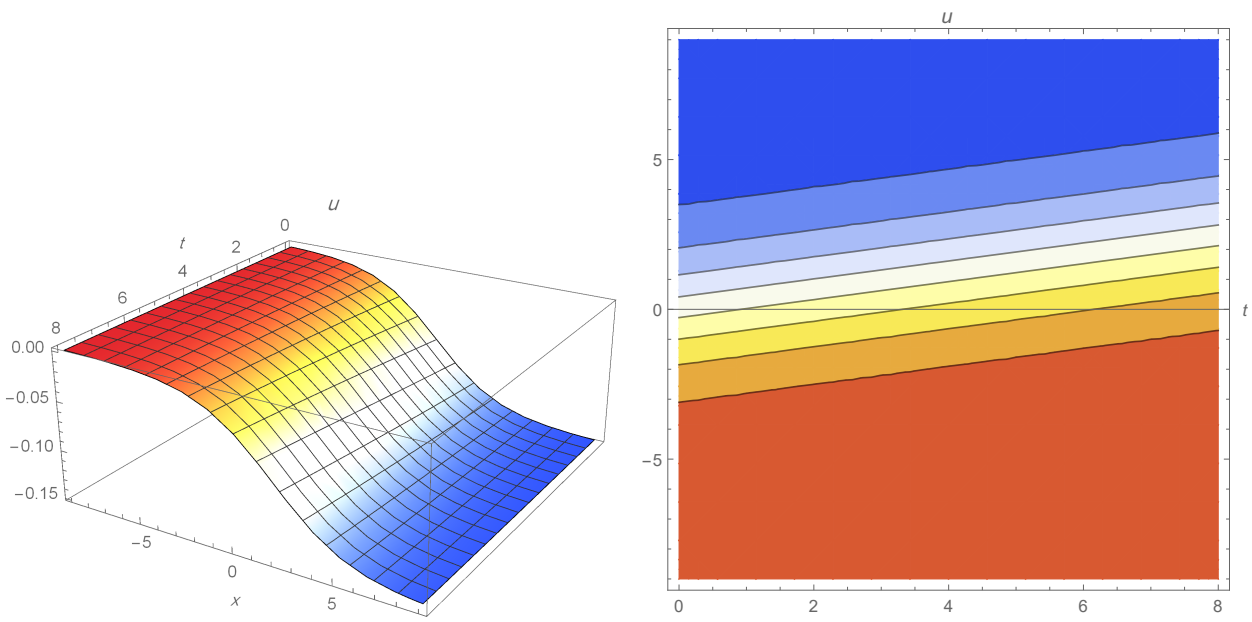

Figure (3): Dark soliton solution of Eq.(3.15).

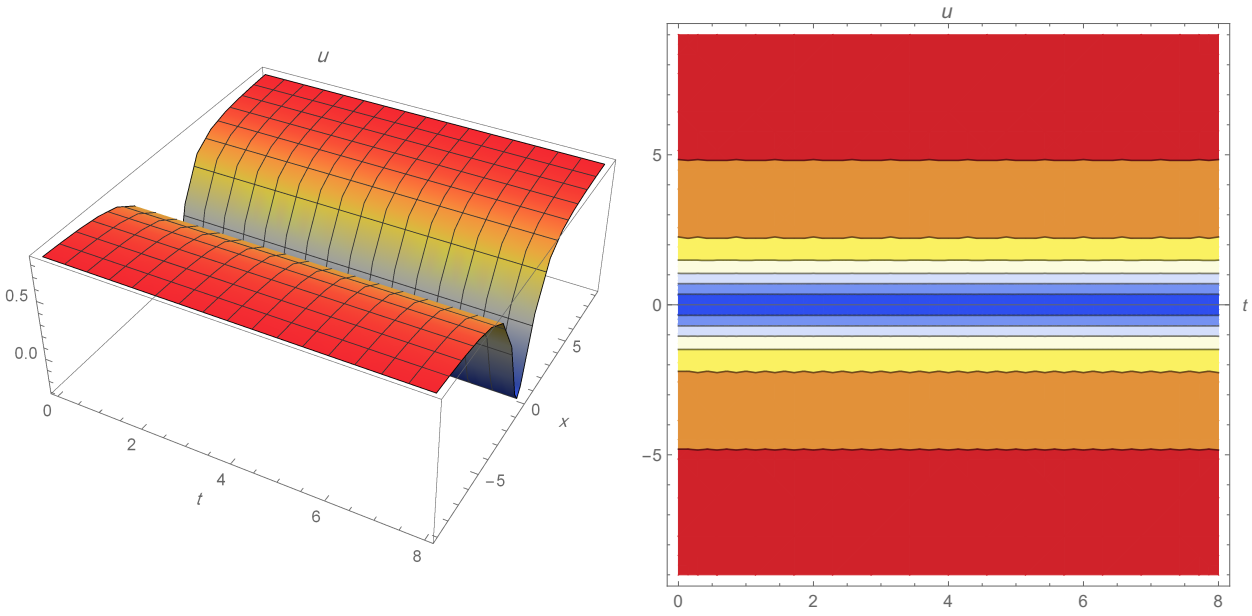

Figure (4): Rational solution of Eq.(3.11).

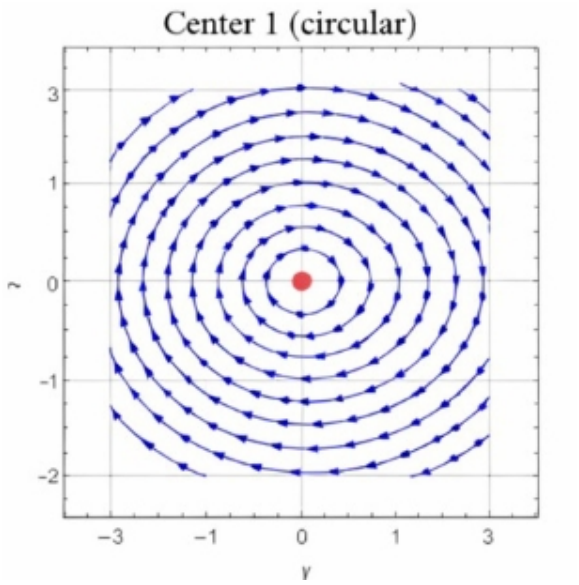

(a)

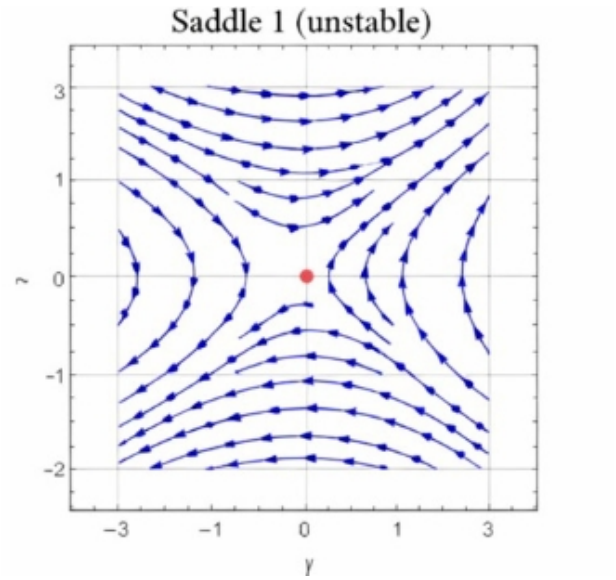

(b)

Figure (5): (a) For $c = 0.155$, $g = -0.5$, and $\rho = 1$ with $\frac{4c}{g} < 0$, the system exhibits a center equilibrium point with closed periodic orbits indicating neutral stability.
(b) For $c = 0.155$, $g = 0.5$, and $\rho = 1$ with $\frac{4c}{g} > 0$, the system exhibits a saddle equilibrium point with separatrix curves indicating instability.

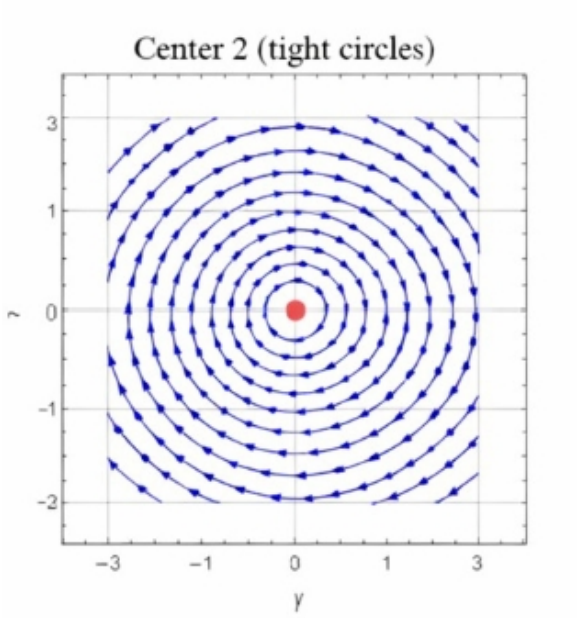

(a)

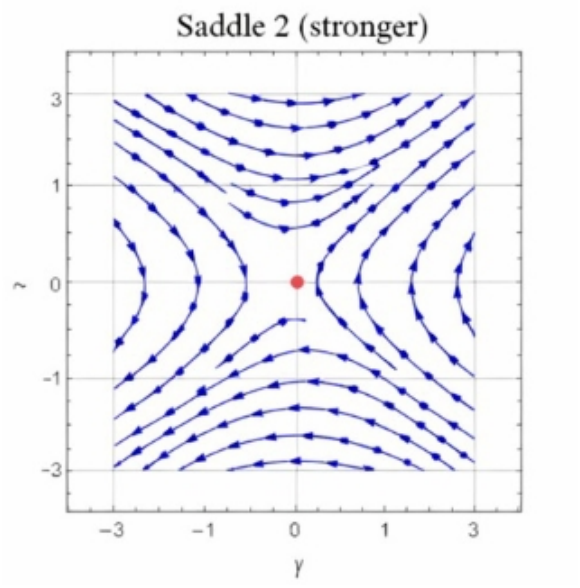

(b)

Figure (6): (a) For $c = 0.1, g = 0.4, \rho = 1$ showing a center equilibrium point. The eigenvalues are purely imaginary and the trajectories form closed periodic orbits, indicating neutral stability.
(b) For $c = 0.1, g = 0.4, \rho = 1$ showing a saddle equilibrium point. The eigenvalues are real with opposite signs, and the trajectories form separatrix curves, indicating instability.

6. Conclusion

In this study, the Modified Extended Mapping Method and its variants were successfully implemented to explore the Higher-Order Boussinesq (HOBB) equation. By employing an appropriate traveling wave transformation, the governing nonlinear partial differential equation is reduced to an ordinary differential equation, facilitating the derivation of a broad spectrum of exact analytical solutions. These solutions encompass various wave morphologies, such as bright, dark, and singular solitons, depending on the specific parameter configurations.

The findings highlight the Modified Extended Mapping Method as a robust and efficient analytical tool for generating diverse solution families for nonlinear evolution equations. Furthermore, the physical characteristics and dynamical evolution of the obtained solutions were visualized using three-dimensional graphical representations, which validated their stability and behavior.

The framework utilized in this study can be readily extended to other nonlinear models in fluid dynamics, nonlinear optics and plasma physics. Prospective studies could extend this methodology to investigate higher-dimensional systems, variable-coefficient models or fractional-order nonlinear evolution equations. Additionally, the integration of bifurcation analysis in this work offered a deeper insight into the equilibrium structures and stability profiles, confirming the potency of this combined approach in deciphering complex nonlinear dynamics.

Conflicts of Interest: The author declares that there are no conflicts of interest regarding the publication of this paper.

References

[1] K.K. Ahmed, N.A. Alsahafi, H.M. Ahmed, S. Boulaaras, M.S. Osman, Diverse Solitons Wave Structures for Coupled NLSEs in Birefringent Fibers with Higher Nonlinearities Using the Modified Extended Mapping Algorithm, Sci. Rep. 15 (2025), 17047. https://doi.org/10.1038/s41598-025-00668-1.

[2] I. Onder, H. Esen, M. Ozisik, A. Secer, M. Bayram, Optical Soliton Solutions of Complex Ginzburg–Landau Equation with Triple Power Law and Modulation Instability, Opt. Quantum Electron. 56 (2024), 1000. https://doi.org/10.1007/s11082-024-06897-4.

[3] M. Shakeel, X. Liu, S. Muhammad, B. Ceesay, Dynamical Behavior of Optical Solitons Propagation in Coupled NLS Equations, Bound. Value Probl. 2025 (2025), 151. https://doi.org/10.1186/s13661-025-02134-3.

[4] E.H.M. Abdullah, H.M. Ahmed, A.A.S. Zaghrout, A.I.A. Bahnasy, W.B. Rabie, Dynamical Structures of Optical Solitons for Highly Dispersive Perturbed NLSE with β-Fractional Derivatives and a Sextic Power-Law Refractive Index Using a Novel Approach, Arab. J. Math. 13 (2024), 441–454. https://doi.org/10.1007/s40065-024-00486-9.

[5] I. Samir, N. Badra, N.S.E. Abdalla, M. Ramadan, H.M. Ahmed, Analytical Characterization of Optical Solitons and Bifurcation Analysis for the (2+1)-D Wazwaz-Kaur Boussinesq Equation, Sci. Rep. 15 (2025), 41762. https://doi.org/10.1038/s41598-025-23216-3.

[6] A.R. Seadway, A. Ali, A. Bekir, A.C. Cevikel, Analysis of the (3+1)-Dimensional Fractional Kadomtsev–Petviashvili–Boussinesq Equation: Solitary, Bright, Singular, and Dark Solitons, Fractal Fract. 8 (2024), 515. https://doi.org/10.3390/fractalfract8090515.

[7] S. Muhammad, A. Saboor, M. Shakeel, H.G. Ahmadzai, Investigation of Optical Soliton Solutions for the Fractional-Order Nonlinear Schrödinger Equation Including Parabolic Law of Nonlinearity, Bound. Value Probl. 2025 (2025), 154. https://doi.org/10.1186/s13661-025-02148-x.

[8] A. Zafar, M. Shakeel, A. Ali, L. Akinyemi, H. Rezazadeh, Optical Solitons of Nonlinear Complex Ginzburg–Landau Equation via Two Modified Expansion Schemes, Opt. Quantum Electron. 54 (2021), 5. https://doi.org/10.1007/s11082-021-03393-x.

[9] N. Das, S. Saha Ray, Investigations of Bright, Dark, Kink-Antikink Optical and Other Soliton Solutions and Modulation Instability Analysis for the (1+1)-Dimensional Resonant Nonlinear Schrödinger Equation with Dual-Power Law Nonlinearity, Opt. Quantum Electron. 55 (2023), 1071. https://doi.org/10.1007/s11082-023-05341-3.

[10] Y. Ma, Z. Wang, Kink, Periodic and Solitary Solutions for Coupled Benjamin–Bona–Mahony–KdV System, J. Taibah Univ. Sci. 17 (2023), 2271236. https://doi.org/10.1080/16583655.2023.2271236.

[11] A. Jaradat, M.S.M. Noorani, M. Alquran, H.M. Jaradat, Construction and Solitary Wave Solutions of Two-Mode Higher-Order Boussinesq-Burger System, Adv. Differ. Equ. 2017 (2017), 376. https://doi.org/10.1186/s13662-017-1431-8.

[12] W. Malfliet, The Tanh Method: a Tool for Solving Certain Classes of Nonlinear Evolution and Wave Equations, J. Comput. Appl. Math. 164-165 (2004), 529–541. https://doi.org/10.1016/S0377-0427(03)00645-9.

[13] A. Zafar, M. Ijaz, A. Qaisar, D. Ahmad, A. Bekir, On Assorted Soliton Wave Solutions with the Higher-Order Fractional Boussinesq–Burgers System, Int. J. Mod. Phys. B 37 (2023), 2350287. https://doi.org/10.1142/s0217979223502879.

[14] X. Li, B. Li, J. Chen, M. Wang, Exact Solutions to the Boussinesq-Burgers Equations, J. Appl. Math. Phys. 05 (2017), 1720–1724. https://doi.org/10.4236/jamp.2017.59145.

[15] A.M. Wazwaz, A Variety of Soliton Solutions for the Boussinesq-Burgers Equation and the Higher-Order Boussinesq-Burgers Equation, Filomat 31 (2017), 831–840. https://doi.org/10.2298/FIL1703831W.

[16] X. Gao, Y. Guo, W. Shan, Water-Wave Symbolic Computation for the Earth, Enceladus and Titan: The Higher-Order Boussinesq-Burgers System, Auto- and Non-Auto-Bäcklund Transformations, Appl. Math. Lett. 104 (2020), 106170. https://doi.org/10.1016/j.aml.2019.106170.

[17] F.Y. Liu, Y.T. Gao, Lie Group Analysis for a Higher-Order Boussinesq-Burgers System, Appl. Math. Lett. 132 (2022), 108094. https://doi.org/10.1016/j.aml.2022.108094.

[18] A.M. Mubaraki, R.I. Nuruddeen, K.K. Ali, J.F. Gómez-Aguilar, Additional Solitonic and Other Analytical Solutions for the Higher-Order Boussinesq-Burgers Equation, Opt. Quantum Electron. 56 (2023), 165. https://doi.org/10.1007/s11082-023-05744-2.

[19] M. Kawser, M. Akbar, M. Khan, H.A. Ghazwani, Exact Soliton Solutions and the Significance of Time-Dependent Coefficients in the Boussinesq Equation: Theory and Application in Mathematical Physics, Sci. Rep. 14 (2024), 762. https://doi.org/10.1038/s41598-023-50782-1.

[20] H.H. Hussein, W. Alexan, S.A. Kandil, Innovative Solutions for Lossy Nonlinear Transmission Lines Model Using a Modified Extended Mapping Approach with Fractional Effects, Sci. Rep. 16 (2026), 8623. https://doi.org/10.1038/s41598-026-35652-w.

[21] N.A. Kudryashov, A. Biswas, A.H. Kara, Y. Yildirim, Cubic–Quartic Optical Solitons and Conservation Laws Having Cubic–Quintic–Septic–Nonic Self-Phase Modulation, Optik 269 (2022), 169834. https://doi.org/10.1016/j.ijleo.2022.169834.

[22] K.K. Ahmed, H. Ahmed, N.M. Badra, M. Mirzazadeh, W.B. Rabie, et al., Diverse Exact Solutions to Davey–Stewartson Model Using Modified Extended Mapping Method, Nonlinear Anal. Model. Control 29 (2024), 983–1002. https://doi.org/10.15388/namc.2024.29.36103.

[23] S.M. Islam, M.E. Islam, M.A. Akbar, D. Kumar, The Stretch Coordinate Effect, Bifurcation, and Stability Analysis of the Nonlinear Hamiltonian Amplitude Equation, Partial Differ. Equ. Appl. Math. 13 (2025), 101126. https://doi.org/10.1016/j.padiff.2025.101126.

[24] K. Khan, M.E. Islam, M.A. Akbar, Bifurcation, Stability, and Nonlinear Parametric Effects on the Solitary Wave Profile of the Riemann Wave Equation, Int. J. Theor. Phys. 63 (2024), 150. https://doi.org/10.1007/s10773-024-05683-y.